

Study of the wettability and the corrosion protection of the hybrid silane (3-aminopropyl) triethoxysilane (APTES) and (3-glycidyloxypropyl) trimethoxysilane (GPTMS) film on galvanized steel

Kleber Gustavo da Silva Souza¹, Fernando Cotting²,
Idalina Vieira Aoki³, Franco Dani Rico Amado¹,
Vera Rosa Capelossi¹

¹ Science and Technology Department State University of Santa Cruz, Highway Jorge Amado km 16, CEP: 45662-900, Salobrinho, Ilhéus, Ba, Brazil.

² Department of Chemical Engineering, Federal University of Minas Gerais, Av. Antonio Carlos, 6627, CEP: 31270-901, Belo Horizonte, MG, Brazil.

³ Department of Chemical Engineering, Polytechnic School of the University of São Paulo, Av. Luciano Gualberto, 380, trav.3, CEP: 05508-010, São Paulo, SP, Brazil.

e-mail: gustavo.souza.ht@gmail.com, fernando@deq.ufmg.br, franco.amado@gmail.com, vera.rosa@gmail.com idavaoki@usp.br

ABSTRACT

In this work, the wettability of the galvanized surface pretreated with the hybrid silane APTES/GPTMS film was measured by sessile drop method. The coatings were applied on the substrate from dip-coating method and dried in an oven. The study followed an experimental factorial design, 3^3 , with contact angle as response. The corrosion resistance was evaluated by electrochemical techniques and the surface morphology was characterized by scanning electron microscopy. The wettability results showed the best condition for galvanized steel pretreated with the hybrid silane film for 2:1 APTES:GPTMS ratio, 2% silane concentration and 150 min of hydrolysis time, because the result may be related to a higher rate of hydrolysis of the silanes that is influenced by both the functional group present and by the type and number of hydrolyzed groups, resulting consequently in a higher availability of silanol groups in solution, promoting a greater crosslinking of the film on the metallic substrate.

Keywords: hybrid silane, corrosion, galvanized steel, pretreatment, wettability.

1. INTRODUCTION

The automobile industry, by requiring strict quality criteria, has increasingly used the galvanized steel, because it presents better corrosion resistance than carbon steel [1]. The total "galvanized" coating thickness ranges between 6 μm and 11 μm . The coating is uneven and cracked, consisting of a columnar grain tangle growing from the inner to the surface [2,3].

The galvanized steel is a product of the heat treated galvanized sheet, in other words, steel coated with zinc after heat treatment. The galvanizing process is carried out at high temperatures in any type of steel, being subjected to a heat treatment in melt zinc baths for the formation of protective coating. The post-treatment conditions on the zinc coated steel, depend of the substrate future use and must be carefully selected, since heat treatments at high temperatures can modify the metal structure and properties [4].

The process of galvanizing involves a complexity of phenomena such as the formation of intermetallic phases ($\text{Eta-}\eta$, $\text{Zeta-}\zeta$, $\text{Delta-}\delta$ and $\text{Gamma-}\Gamma$ respectively the outermost to innermost) in the solid/liquid interface and diffusion phase transformations in the solid state. These intermetallic phases have free enthalpy of formation and free energy of formation values very close to each other. The phase growth depends on the temperature and time of thermal treatment, besides on the metal element added to the bath, such as aluminum [5,6].

"Galvanized" coating microstructure shows pores in the Zeta phase (ζ) which growth during the heat treatment process and its porosity allows the entrance of electrolyte and the precipitation of the corrosion products [7]. In order to minimize these electrolyte entrance and thereby reduce the corrosive effect on metal,

a hybrid coating based on silanes APTES [(3-Aminopropyl)triethoxysilane] and GPTMS [(3-Glicidoxypopyl)trimethoxysilane] was applied on the galvanized steel.

The silanes have organic and inorganic chemical properties, hence the name organic-inorganic hybrids, which combine the best properties of inorganic compounds as thermal and chemical stability, with the best properties of organic polymers such as processability and flexibility [8]. The silanes are environmentally friendly; therefore, they are used in the paint industry as a coupling agent between different interfaces and also in pre-treatment of metallic surfaces against corrosion.

The silane film can be applied over many metal alloys previously treated in alkaline solution, by immersing the metal for a few minutes in a dilute solution of silane (no more than 10% of silane) followed by a cure at temperatures between 80-150°C [9-11]. Curing is applied to improve the cross-linking of the film due to formation of covalent bonds [11].

The silane pretreatment have the advantage of forming thin films, being few hundredths of micrometers thick but sufficient to provide good corrosion resistance. A good quality silane film must provide covalent bonds as SiOMetal and SiOSi (siloxanes), forming a homogeneous film without porosity, stable to the atmosphere and presenting many functional groups to bind the subsequent polymeric layer [13].

The formation of the silane film starts from the hydrolysis and condensation reactions of the precursor silanes. These reactions occur simultaneously and are opposed to each other, whose rate of reaction is directly influenced by solution pH. They occur in acid aqueous solutions being the hydrolysis faster than the condensation at such acidic conditions for most of silanes [14,15].

In the hydrolysis reaction the hydrolysable alkoxy groups such as methoxy (-OCH₃) and ethoxy (-OCH₂CH₃) react with water to form the silanol (SiOH) which is responsible for adsorption and anchoring in the wet (alkali activated) metal surface. On the other hand, in condensation reaction the silanol will react itself to form larger molecules, causing a slow polymerization that forms a siloxane compound (SiOSi)_n, which may precipitate on the metal surface forming the protective film or in solution, damaging the quality of the future film to be formed [16,17].

The hydrolysis rate of a silane molecule is influenced by its functional group as the type and number of hydrolysable groups. The hydrolysis rate is high for small hydrolysable alkoxy group. Silanes highly hydrophobic that need larger amounts of ethanol in the solution hydrolyze more slowly. The hydrolysis reaction rate is related to the steric effect of the alkoxy group [18].

The silane films are protective for substrates in which are deposited and so they can form a hydrophobic barrier that reduce the diffusion rate of water and/or electrolyte ions to the metal surface. The silanes hydrophobicity depends on the chemical functional group present in its chain [19,20]. The hydrophobic character of the film can be attributed to contact angles equal or higher than 90°. However, when the silane film is immersed in water or some electrolyte, the contact angle can decrease due to not stable siloxane groups (SiOSi) or to the presence of free silanols groups (SiOH) which are hydrophilic [21,22].

APTES is an organofunctional monosilane in which one side of the structure is supplied with an active group, such as amino and vinyl, which can react with synthetic resin molecules such as epoxy, phenolic, polyester; while in the other side it has an alkoxy group. These groups can react with the hydroxyl groups on the surface of the substrate and generate reactive silicon alcohol in the presence of water (aqueous solution) or air. APTES has been used as a coupling agent for over than 40 years. In addition, it can also be used in the production of plastic reinforced with fiber glass, cotton fiberglass and mineral cotton in order to improve its mechanical strength and resistance to moist environment moreover to increase the compressive strength when added to the phenolic resin binder. It can be used in dental adhesive and to improve the wettability and dispersion of polymer fillers. It also can be used to the immobilized enzyme attached to the surface of glass substrate, to sand control in oil well drilling, to prevent sand from drilling, to brick surface with hydrophobic, to make the fluorescent lamp coating have high surface resistance, and to improve the moisture absorption properties of organic matter on the surface of glass in the medium of liquid chromatography. It is a catalyst in the platinum by the chloroform and alkene with the active group and then obtained by alcoholysis. They can also be used in surface conditioning to obtain devices with reproducible electrical characteristics for molecular detection applications, functionalized as reference devices for biological chemical sensors [23-25].

Currently, there is no clear standard characterization relative to APTES films wetting properties. According to current knowledge of the wettability of the APTES there are at least three factors that can influence. The first is surface hydrogen bonds formed between the droplets of water molecules and amino acid groups present in APTES surface. The second is that the APTES has a rough surface, based on AFM observation [23,26]. This roughness can cause additional surface forces to suppress the contraction of the three-phase contact line [23,26]. Third, studies have shown that the APTES film is not well organized and its struc-

ture is not compact [25,27,28]. Some authors reported that water molecules can penetrate even into a dense organic layer if the hydrophobic chains are too short, which can induce deformation of the organic layer and result in additional force on the sample [29,30]. When a drop enters in contact with a "virgin" surface for the first time, a short period of time could be necessary to get balance between the drop and the surface. Due to the influence of surface hydrogen bonding, surface roughness, water penetration effects, the droplet profile in the three-phase contact line can be deviated from the mass drop profile, and the authenticity of the angles calculated by various methods could be questionable. [23].

GPTMS is a bifunctional organosilane with three methoxy groups on one side of the structure and one epoxy group on the other side. Like other organosilanes, GPTMS is easily hydrolyzable, and methoxy groups are substituted by hydroxyl groups to form a trisilanol [31]. They have been widely studied as coupling agents in multi-walled carbon nanotubes and polymer nanocomposites to improve the mechanical properties, especially the increase in elasticity modulus and flexure, wear and thermal resistance, with increasing glass transition temperature (T_g) of the matrix [32,33]. The GPTMS silane is used to functionalize carbon nanotubes with multiple walls for the reinforcement of epoxy matrix, with the advantage that the presence of the epoxy in its structure favors the physical interaction between the GPTMS nanotubes and the epoxy groups of the resin and there is the possibility of a chemical bond between the GPTMS nanotubes and the hardener, thus that is woven throughout the network of polymer chains [31,34]. GPTMS is also used to optimize as well as to ensure compatibility with epoxy resin [35]. Another use of GPTMS is in conducting polymers, in order to achieve stability in polar solvents, it is typically used for Poly (3,4- Ethylenedioxythiophene) doped with poly (styrene sulfonate), avoiding dissolution and delamination, but also the excess could lead to reduce load mobility, reduction conductivity [36,37]. The surface wettability reflects the affinity of the surface with water and the measurements of its angles are performed to determine the wetting properties of the film. Thus, on the wettability of the GPTMS, the epoxide ring opening reaction, which is catalyzed by acid. For example, phosphonic acid may form diols, alcoholic alkoxy and polyether products. The diols add hydrophilicity to the silica surface due to their high hydroxyl content [37-39].

This work aims to analyze the surface wettability of the APTES/GPTMS hybrid silane film as pre-treatment on galvanized steel in order to improve this anticorrosive surface treatment. The experiments were planned based on a factorial experimental design, 3^3 , with the contact angle as response. The three studied variables were: ratio of APTES:GPTMS (1:2, 1:1 e 2:1), concentration of silanes (2%, 4% e 6% volume %) and time of hydrolysis (30 min, 90 min e 150 min) at three levels. The validation of the experimental design was evaluated by statistical analysis. The morphological surface characterization was carried out by scanning electron microscopy (SEM) and energy dispersive spectroscopy (EDS). The corrosion resistance was evaluated by electrochemical techniques, as open circuit potential (OCP) and electrochemical impedance spectroscopy (EIS).

2. EXPERIMENTAL

The research was conducted using a factorial experimental design, 3^3 , with three variables at three levels as presented in Table 1.

Table 1: Experimental Factorial design 3^3 .

Variables	Levels			
	L1(-1)	L2(0)	L3(+1)	
Ratio of (APTES:GPTMS)	(V1)	1:2	1:1	2:1
Silane concentration (volume %)	(V2)	2%	4%	6%
Hydrolysis time	(V3)	30 min	90 min	150 min

The development of the factorial experimental design was carried out according to the variables presented in Table 2.

Table 2: Matrix of experiments for the 3^3 design with three independent variables at three levels.

Samples (S)	V1		V2		V3	
SBlank	----	----	----	----	----	----
S01	1:2	(-1)	2%	(-1)	30 min	(-1)

S02	1:1	(0)	2%	(-1)	30 min	(-1)
S03	2:1	(+1)	2%	(-1)	30 min	(-1)
S04	1:2	(-1)	4%	(0)	30 min	(-1)
S05	1:1	(0)	4%	(0)	30 min	(-1)
S06	2:1	(+1)	4%	(0)	30 min	(-1)
S07	1:2	(-1)	6%	(+1)	30 min	(-1)
S08	1:1	(0)	6%	(+1)	30 min	(-1)
S09	2:1	(+1)	6%	(+1)	30 min	(-1)
S10	1:2	(-1)	2%	(-1)	90 min	(0)
S11	1:1	(0)	2%	(-1)	90 min	(0)
S12	2:1	(+1)	2%	(-1)	90 min	(0)
S13	1:2	(-1)	4%	(0)	90 min	(0)
S14	1:1	(0)	4%	(0)	90 min	(0)
S15	2:1	(+1)	4%	(0)	90 min	(0)
S16	1:2	(-1)	6%	(+1)	90 min	(0)
S17	1:1	(0)	6%	(+1)	90 min	(0)
S18	2:1	(+1)	6%	(+1)	90 min	(0)
S19	1:2	(-1)	2%	(-1)	150 min	(+1)
S20	1:1	(0)	2%	(-1)	150 min	(+1)
S21	2:1	(+1)	2%	(-1)	150 min	(+1)
S22	1:2	(-1)	4%	(0)	150 min	(+1)
S23	1:1	(0)	4%	(0)	150 min	(+1)
S24	2:1	(+1)	4%	(0)	150 min	(+1)
S25	1:2	(-1)	6%	(+1)	150 min	(+1)
S26	1:1	(0)	6%	(+1)	150 min	(+1)
S27	2:1	(+1)	6%	(+1)	150 min	(+1)

The organosilanes APTES [(3-aminopropyl)triethoxysilane] (purity $\geq 98\%$) and GPTMS [(3-Glycidyoxypropyl)trimethoxysilane] (purity $\geq 98\%$) were obtained from Sigma-Aldrich and their molecular structure are presented in Figure 1.

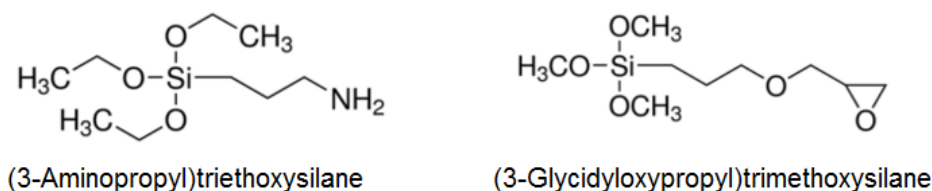


Figure 1: Molecular structure of silanes. Supplier Sigma-Aldrich.

2.1 Samples preparation

The galvanized steel was supplied by Usiminas (the chemical composition of galvanized, according USIMINAS, in weight % is approximately 0.003 C, 0.2 Mn, 0.009 S, 0.008 P, 0.05 Si, 0.029 Al, 0.012 Ti, 0.0022 N, 90 Zn and 10 Fe. The galvanneal coatings contain 9-12% bulk Fe, with between 0.20 and 0.50% bulk Al). The samples were cut in dimensions of 25 x 25 x 0.9 mm. The samples were manually cleaned using ethanol, washed with distilled water and dried with hot air. After that, the samples were immersed in acetone and submitted to an ultrasound bath for 10 min, washed with distilled water and dried. Then the samples were degreased in alkaline degreaser N667 Saloclean (5% aqueous solution) for 10 min at 55°C to create OH groups in the metal's surface and then washed in distilled water and dried.

2.2 Silanes solution

A solvent composed of distilled water and ethanol (50% / 50% v/v) was prepared and its pH = 4 was adjusted with glacial acetic acid because it does not interfere directly in the hydrolysis for being a weak acid and high volatility [40,41]. At this pH the hydrolysis rate is high and the condensation is minimal, resulting in a solution rich in silanols (Si-OH) which are the agents responsible for adhesion to the metal substrate [9,42].

The APTES silane was added to the solvent solution, under stirring, followed by addition of GPTMS silane. The total volume of both silanes corresponds to the desired volume % in relation to the total solution volume. The silane concentration and hydrolysis time are reported in Table 2. The hydrolysis was conducted under stirring at room temperature.

2.3 Deposition of hybrid silane film (silanization) and its cure

After hydrolysis of silanes, the metallic samples were immersed in the hydrolyzed solution and maintained for 25 min by a dip-coating process manually immersed controlled, under low stirring, at room temperature. The long immersion time of galvanized steel in the hydrolyzed solution is necessary to the formation of a compact and homogeneous silane film due to the natural porous surface of the galvanized, which results from thermal treatment of the zinc coating [19]. After the silanization process, the samples were cured for 60 min at 150 °C in an oven.

2.4 Scanning Electron Microscopy (SEM) and Energy Dispersive Spectroscopy (EDS)

The morphology of galvanized steel surface with and without silane film was analyzed by SEM - operated at 5 kV with secondary electrons - and EDS in Quanta 250F microscope. The samples with and without pre-treatment were analyzed before and after 24 h of immersion in 0.1 mol/L NaCl. Before SEM analysis the samples were dried at room temperature. All the samples were gold coated by an automatic sputter-coated.

2.5 Contact Angle Measurement (Wettability Test)

The contact angle measurements were performed in the DataPhysics OCA 15plus equipment with SCA20 software at 18 °C. The measurements were performed through the sessile drop method. The equipment was calibrated by measuring the surface tension of water/air. There were performed three contact angle measurements for each sample treated and untreated. The measurements were performed in the center of each sample. The contact angle values were registered 10 seconds after depositing a drop of deionized water, with a volume of approximately 12 µL, on the samples surface.

2.6 Electrochemical Tests

Electrochemical tests were acquired in the AUTOLAB PGSTAT302N model potentiostat and data were acquired by NOVA 1.11 software. For the electrochemical data treatment Microcal® Origin® 8.0 software were used.

The electrochemical measurements were performed in electrochemical cell with three electrodes with Ag|AgCl|KCl_{sat} as reference electrode, titanium (Ti) wire coated with rhodium (Rh) as auxiliary electrode and galvanized steel with exposed area of 1 cm² as working electrode. The electrolyte used was an aqueous solution 0.1 mol/L NaCl. The electrochemical tests were performed in aerated and unstirred electrolyte. The electrochemical impedance spectroscopy (EIS) measurements were acquired at the open circuit potential (OCP) after 90 min of stabilization, from 100 kHz to 10 mHz, with 10 points per frequency decade using a potential perturbation amplitude of 10 mV (rms). The linear polarization resistances (R_p) were acquired subsequently to EIS measurements, from ±20 mV vs OCP at scan rate of 0.167 mV s⁻¹. The potentiodynamic polarization curves were obtained after R_p measurements and the Tafel curves were performed from ±250 mV vs OCP at scan rate of 0.5 mV s⁻¹.

3. RESULTS AND DISCUSSION

3.1 Scanning Electron Microscopy (SEM) and Energy Dispersive Spectroscopy (EDS)

The surface morphology of galvanized steel was analyzed by SEM. Figure 2 presents the SEM images for galvanized steel without silane film (SBlank) and SBlank after 24 h of immersion in 0.1 mol/L NaCl solution.

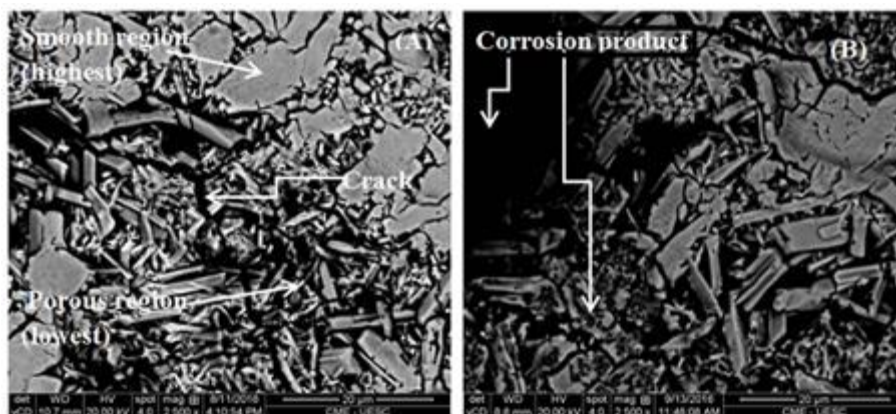


Figure 2: SEM images for galvanized steel without silane film (SBlank) before (A) and after (B) 24 h of immersion in 0.1 mol/L NaCl solution.

The galvanized surface presents different areas (Fig.2 A), ones smoother and outer layers rich in zinc (Eta phase), and others porous, which are inner and show the intermetallic phases [19,43]. The crack is related to Zeta phase (ζ), which presents a higher Zn than Fe concentration, due to be nucleated first and then grows epitaxially on the substrate at a high rate [19,43]. Cook & Grant [2] and Almeida & Morcillo [3] declare that the "galvanized" is uneven with cracks and a columnar grain tangle which grows from inside the coating to the surface (Fig. 2A).

Figure 2B shows that corrosion products have predominance in porous region. According to Queiroz and Costa [7], the pores derived from Zeta phase (ζ) growth, allow the electrolyte penetration and formation of corrosion products, thus explaining the notable presence of this products in the attacked sample.

Figure 3 presents the SEM images of galvanized steel pretreated with silane film (2:1 silane ratio APTES:GPTMS, 2% silane concentration and 150 min hydrolysis time) before (Fig 3A) and after 24 h of immersion in 0.1 mol/L NaCl solution (Fig. 3B).

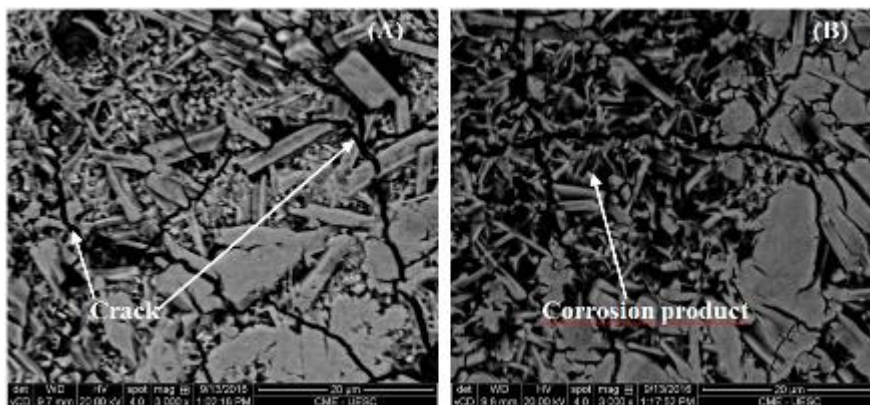
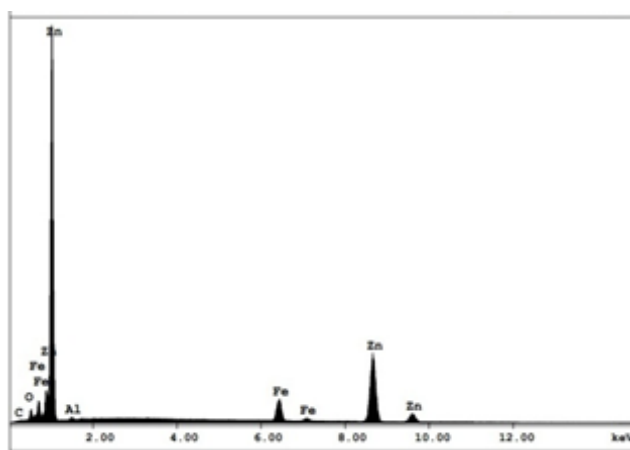
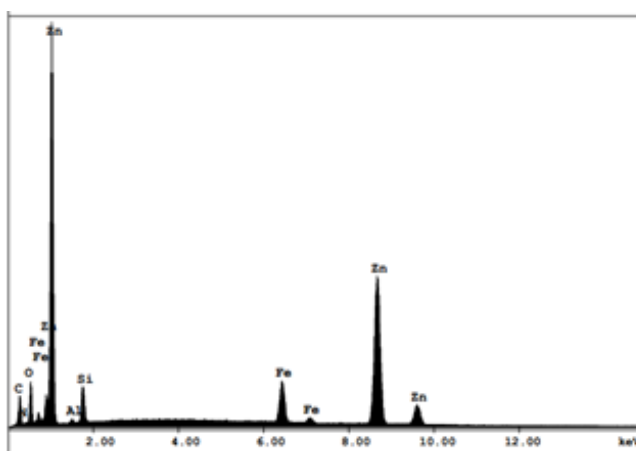


Figure 3: SEM images of the galvanized steel with silane film before (A) and after (B) 24 h of immersion in 0.1 mol/L NaCl solution.

Comparing Fig 2B and Fig 3B it is observed that the sample pretreated with silane film is less attacked than the SBlank indicating the silane film protection role. On the other hand, comparing Fig 2A and Fig 3A no difference is observed, however, the EDS images (Fig 4) of these samples reveals the presence of silane film due to the presence of Si and N (APTES aminofunctional group) peaks (Fig 4B) while in Fig 4A there is only Zn and Fe peaks which is characteristic of the bare galvanized surface.



(A)



(B)

Figure 4: EDS images for galvanized steel in the smooth region without silane film (SBlank) (A) and with silane film (B).

The SEM images and EDS results indicate that the galvanized microstructure can contribute with the non-homogeneous film formation due to the surface porosity originating from intermetallic phases and the presence of cracks [4-7, 14,19]

Figure 5 shows the SEM of the sample profile S21 with the indication of the thickness of the galvanneal coating and the silane hybrid film. The galvanneal coating has a thickness of approximately 7 μm , while the silane hybrid film has a thickness of approximately 2.5 μm .

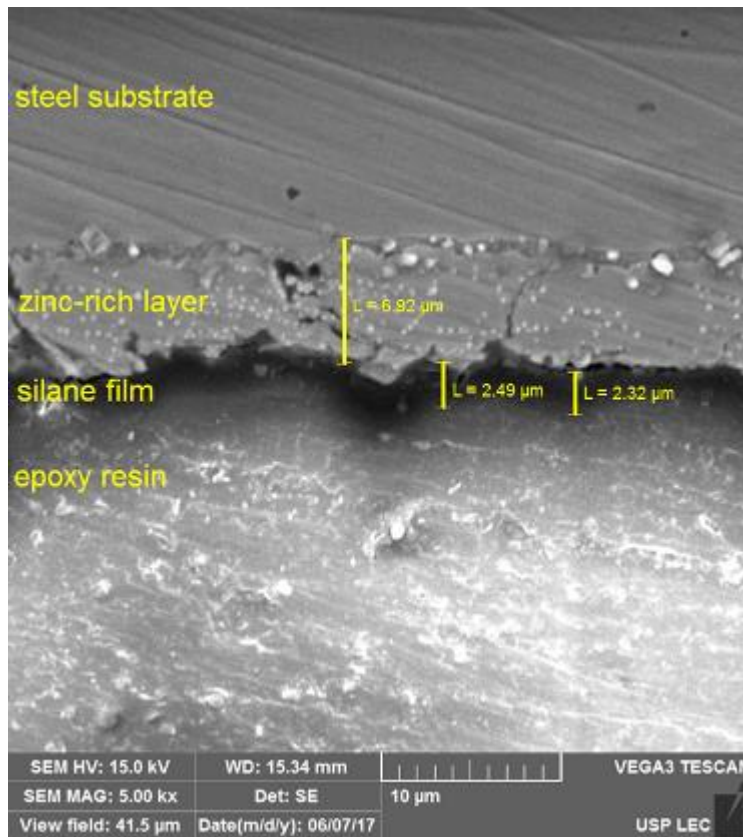


Figure 5: SEM micrograph of the cross-section galvanized steel with silane film for thickness identification.

3.2 Wettability Test (Contact Angle)

The contact angle measurements for galvanized steel treated with silane APTES/GPTMS film and untreated sample (SBlank) are presented in Table 3.

Table 3: Contact angles for samples with and without silane film.

Sample	Measurements			Mean (°degrees)	Standard deviation
	1	2	3		
SBlank	57.8	61.6	60.1	59.8	1.9
S01	103.4	106.9	101.3	103.9	2.8
S02	109.9	106.2	101.6	105.9	4.2
S03	102.4	97.3	99.7	99.8	2.6
S04	75.3	67.2	66.7	69.7	4.8
S05	90.7	93.3	96.2	93.4	2.8
S06	89.7	84.8	86.2	86.9	2.5
S07	71.0	62.4	65.1	66.2	4.4
S08	81.1	73.7	76.8	77.2	3.7
S09	82.9	75.7	75.3	78.0	4.3
S10	85.6	84.0	107.1	92.2	12.9
S11	93.7	88.3	88.5	90.2	3.1
S12	81.5	85.0	83.3	83.3	1.8
S13	65.4	70.1	71.4	69.0	3.2
S14	75.4	77.6	74.8	75.9	1.5
S15	77.3	79.3	75.5	77.4	1.9
S16	69.7	68.5	63.0	67.1	3.6
S17	80.6	74.5	74.7	76.6	3.5
S18	68.5	72.0	76.8	72.4	4.2
S19	82.5	79.2	79.2	80.3	1.9
S20	72.7	74.7	75.6	74.3	1.5
S21	108.7	112.0	108.4	109.7	2.0
S22	79.0	78.6	75.7	77.8	1.8
S23	73.8	76.7	72.3	74.3	2.2
S24	104.4	93.4	99.6	99.1	5.5
S25	66.7	68.1	70.1	68.3	1.7
S26	88.0	89.0	78.5	85.2	5.8
S27	77.3	80.0	74.6	77.3	2.7

The average contact angle of the untreated sample was 59.8° indicating that the untreated surface is hydrophilic as reported in the literature [19,43,44]. However, all samples treated with silane film presented an average contact angle greater than the SBlank. On the other hand, S21 (ratio 2:1 APTES:GPTMS, 2% silane concentration and hydrolysis time 150 min) was the sample with higher average contact angle (109.7°) being its surface considered as hydrophobic due to its contact angle value higher than 90° [19,45]. In addition to this, other samples presented the hydrophobic character, as highlighted in Table 3. In opposition, S07 (ratio 1:2 APTES:GPTMS, silane concentration of 6% and hydrolysis time 30 min) was the pretreated sample that showed lower average contact angle 66.2° indicating its hydrophilic surface (Table 3).

The rate of hydrolysis of a silane molecule is influenced by both the functional group present and by the type and number of hydrolyzed groups. Highly hydrophobic silanes that need larger amounts of alcohol in solution hydrolyze more slowly. According to Zhu (2005), the smaller the size of the hydrolysable alkoxy group greater is its rate of hydrolysis. This rate of hydrolysis reaction is associated with the steric effect of this alkoxy group. According to Montemor and Ferreira [21], the concentration of silane in the solvent is an important parameter in the pre-treatment process based on silanes. The more hydrolysable groups the silane has,

greater the tendency to arise silanol groups (SiOH), which in addition to reacting with hydroxyls present on the surface of the metal forming the bond (MeOSi), react with each other by polymerizing, condensing in (SiOSi)-n to form the film.

From results obtained from the mean contact angle values (Table 3), it can be seen that a higher epoxy silane ratio (2:1 APTES:GPTMS), a lower silane concentration (2 %) and higher hydrolysis time (150 min) provided higher surface hydrophobicity. This combination of factors, associated with the best results, may be related to a higher rate of hydrolysis of the silanes and consequently higher availability of silanol groups present in solution, as also a higher concentration of epoxy functional groups, which promotes a greater cross-linking of the film on the metallic substrate [17,21,45].

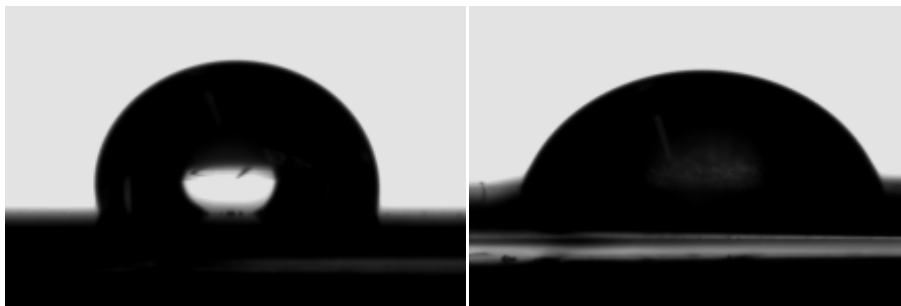


Figure 6: Water drop during the wettability test on galvanized steel with silane hybrid film in the higher (S21) and lower (S07) contact angle value.

3.3 Statistical Analysis

The contact angle (response variable) data were treated by Statistica 10 software, in order to verify the effect of three independent variables (silanes ratio, silane concentration and hydrolysis time) in three levels each one (Table 1). Table 4 presents the values of the model regression coefficients, the effects of the independent variables and all its linear and quadratic relationships for the contact angle response variable.

Table 4: Model regression coefficients and effects of the variables: Ratio (APTES: GPTMS), silane concentration and hydrolysis time for the contact angle response.

	effect	t-value	p-value	coef.
Constant term	82,6	52,6	0,00	82,64
V1	9,9	2,6	0,03	4,97
V1 ²	1,5	0,5	0,66	0,77
V2	-19,0	-4,9	0,00	-9,52
V2 ²	-3,4	-1,0	0,34	-1,69
V3	-3,9	-1,0	0,35	-1,93
V3 ²	-6,6	-2,0	0,08	-3,31
V1.V2	1,6	0,3	0,74	0,81
V1.V2 ²	4,3	1,0	0,33	2,14
V1 ² .V2	6,4	1,6	0,15	3,21
V1 ² .V2 ²	-0,2	-0,1	0,95	-0,12
V1.V3	5,8	1,2	0,25	2,90
V1.V3 ²	-6,3	-1,5	0,16	-3,13
V1 ² .V3	-7,8	-1,9	0,09	-3,89
V1 ² .V3 ²	1,9	0,5	0,62	0,93
V2.V3	9,1	1,9	0,09	4,56
V2.V3 ²	1,9	0,5	0,66	0,94
V2 ² .V3	3,2	0,8	0,46	1,60
V2 ² .V3 ²	-2,1	-0,6	0,57	-1,06

The lower the p-value parameter is, it represents the probability of each independent variable of the experimental factorial design of being significant to the model. In this context, the significant variables are the linear variables V1 (ratio APTES:GPTMS) and V2 (silane concentration), that presents a significance level of 0.05 (95% confidence) or smaller p-value. The variable 1 (ratio APTES:GPTMS) showed significant positive effect (Table 4), indicating that a higher independent variable value implies in the higher value of contact angle, while the variable 2 (silane concentration) showed significant negative effect (Table 4), indicating that a higher independent variable value implies in a lower value of contact angle. It must be stressed that variable V2 has more intense effect when compared to variable 1, so the silane concentration plays a more and intensive effect on the hydrophobicity of the obtained hybrid film. The mathematical model was established for contact angle taking in account only the significant variables due to their low p-values, being Θ_{est} the estimated value of contact angle for the model (Eq. 1).

$$\Theta_{est} = 82.64 + 4.97V_1 - 9.52V_2 \quad \text{Eq.(1)}$$

The model determination coefficient of $R^2 = 0.87$ means that 87.01% of experimental data can be considered obeying the model. According to literature, confidence levels higher than 80% can be considered significant to the model [48-50].

Figure 7 represents the Pareto diagram which shows the t-value of the regression coefficient with 95% confidence. The significance level p, lower than 0.05, indicates ratio (APTES:GPTMS) (V1) and silane concentration (V2), this with a higher effect, as being significant variables for model with 95% probability of significance, strongly interfering in the wettability of the film formed on the substrate.

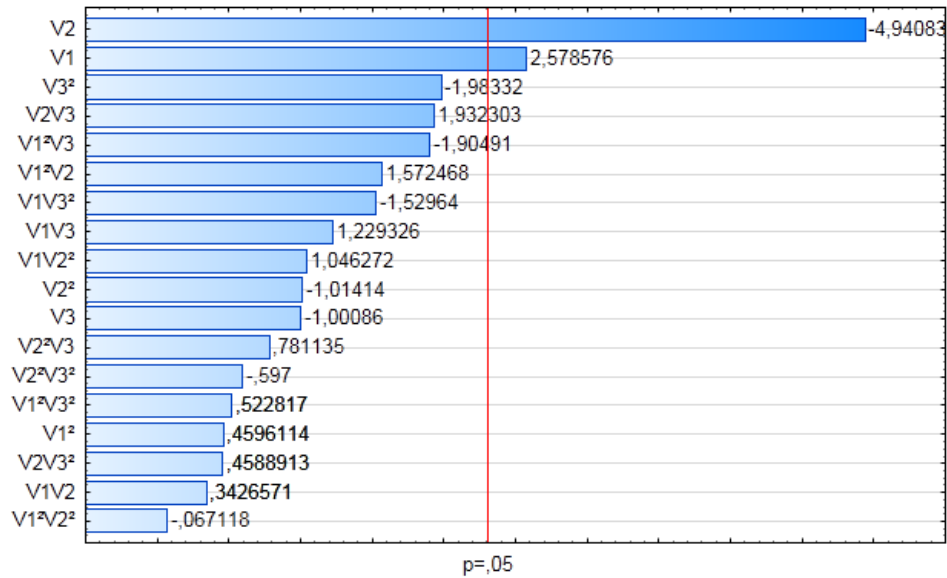


Figure 7: Pareto for contact angle response according to the coded variables

The linear regression between the observed and predicted values is presented in Figure 8. The determination coefficient (R^2) value is 87.01% indicating the proximity of the experimental data and the model (Θ_{est}) revealing how the model is significant [48-50]. It is possible to observe the distribution between predicted and observed values with a greater concentration of points between 66° and 79° for observed and between 64° and 84° for predicted values.

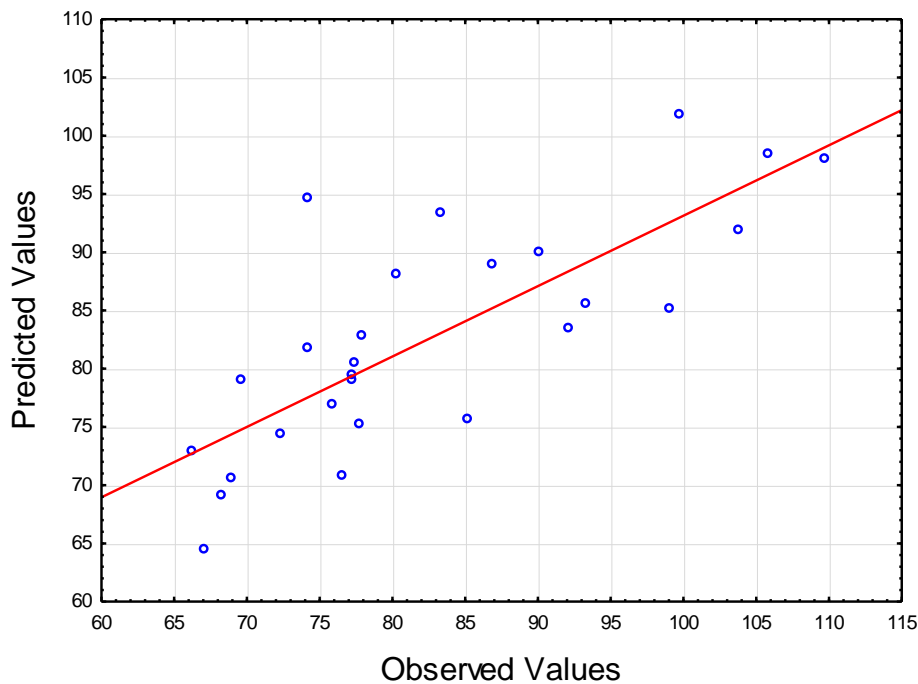


Figure 8: Predicted and observed values for real impedance (Z') as response.

Figure 9 presents the contact angle surface response as function of silane ratio and silane concentration, being hydrolysis time (non-significant variable) at the midpoint (level 0) corresponding to 90 min. It is verified that the higher contact angle values are obtained for low levels of silane concentration tending to 2% (points -0.8 to -1.2) independent of the silane ratio, thus the hydrophobic character (angle $> 90^\circ$) is strongly related to 2% of silane concentration (point -1.2) and has the higher value observed for the contact angle, when the hydrolysis time is 90 min, tending to a ratio 2:1 APTES:GPTMS (point +1.2)

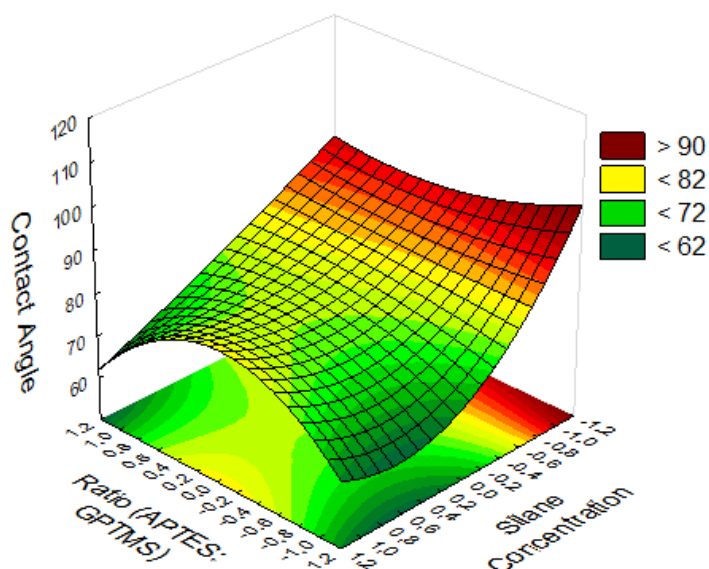


Figure 9: Contact angle response surface as function of silane concentration (V2) and ratio (APTES: GPTMS) (V1) for 90 min hydrolysis time.

The statistic validation of experimental factorial design revealed that the contact angle results and model proposed are reliable ($R^2 = 0.87$). According to the literature coefficients of determination greater than 80% are reliable models [48-50]. It was determined that the variables which great influence in the formation of the film studied are silane concentration (V2) (strongest effect) and silane ratio (V1).

3.4 Electrochemical Characterization

3.4.1 Open Circuit Potential (OCP)

The OCP for galvanized steel treated with silane hybrid film and untreated were obtained after 90 min of immersion in 0.1 mol/L NaCl solution. The OCP curves for galvanized untreated (SBlank), galvanized pretreated with higher (S21) and lower contact angle (S07) values are presented in Figure 10.

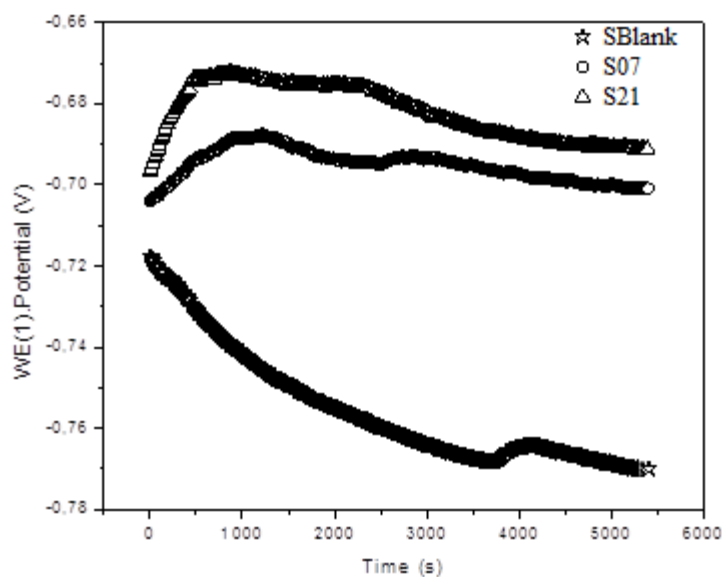


Figure 10: OCP monitoring with time for galvanneated steel with and without silane hybrid film in the higher (S21) and lower (S07) contact angle value, obtained after 90 min of immersion in 0.1 mol/L NaCl solution.

Figure 10 shows that the potential values for the treated galvanneated steel grows in the initial times of immersion due to the film resistance against the electrolyte penetration. The interfacial reactions reach equilibrium (corrosion potential stabilization) in more positive potentials, indicating that the film formed in the substrate is resistive, reticulated and homogeneous [1,48,50].

3.4.2 Electrochemical Impedance Spectroscopy (EIS)

The EIS Bode diagrams, obtained after 100 min of immersion in 0.1 mol/L NaCl for galvanneated untreated and treated with silane hybrid film with higher (S21) and lower (S07) contact angle values are showed in Figure 10. The Bode diagram, impedance modulus value (Fig. 11A), indicate that both samples (S21 and S07) present a higher impedance modulus values than SBlank; on the other hand, the Bode diagram phase angle (Fig. 11B) reveals the presence of two time constants (for sample S07), one at high frequencies which is related to the silane hybrid film response and other at low frequencies due to interfacial reactions galvanneated/electrolyte [19,44]. However, in the intermediate frequencies it is observed a non-capacitive behavior (Fig. 11A) and a new time constant seems to appear (Fig. 11B) for S07 if compared with S21 behavior, which can indicate that the film formed for S07 is less reticulated and homogeneous and resistive than the film formed for S21, thus justifying its lower contact angle value obtained in the wettability tests (Table 3). It is also possible to observe the better barrier layer of S21 in a large range of intermediate frequencies (Fig. 11B), indicating the higher film resistance to interfacial reactions [44,50].

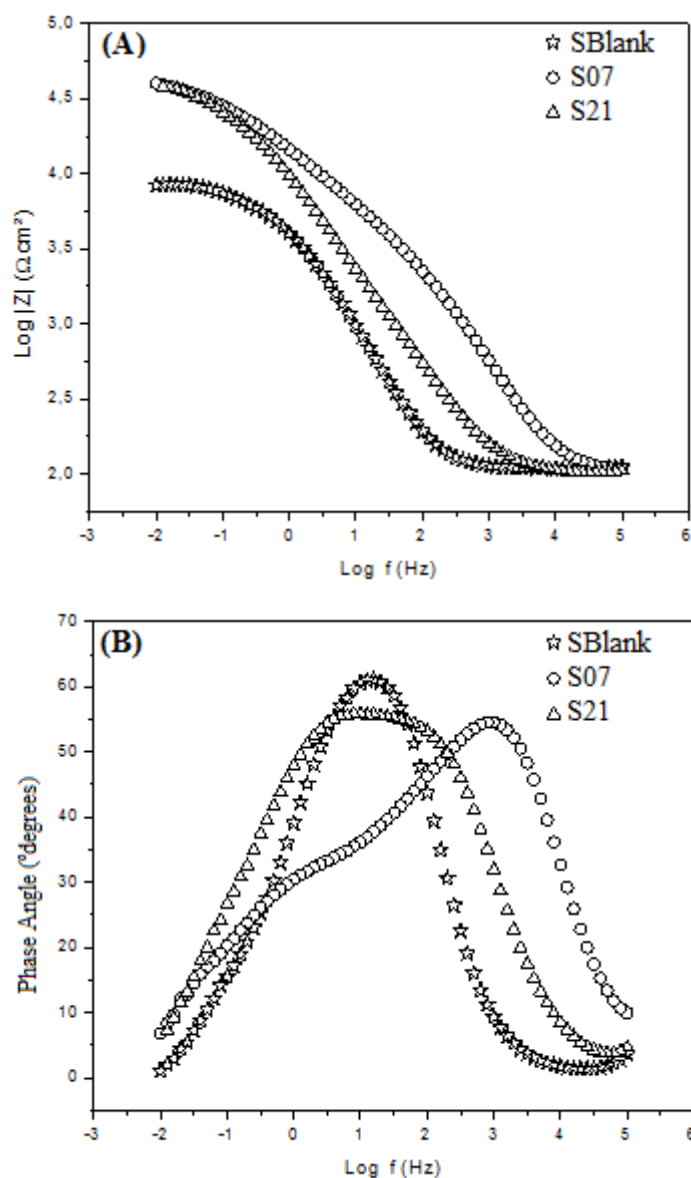


Figure 11: EIS Bode diagrams for the galvanneated untreated and treated with the higher (S21) and lower (S07) contact angle value, obtained after 100 min of immersion in 0.1 mol/L NaCl solution. Bode diagram impedance modulus (A) and Bode diagram phase angle (B).

The electrochemical results corroborate the wettability results indicating that the silane hybrid film (APTES/GPTMS) improves the galvanneated corrosion resistance.

4. CONCLUSIONS

The statistical analysis of experimental factorial design revealed that the contact angle results and proposed model are significant ($R^2 = 0.87$). It was determined that the variables which has great influence in the formation of the hybrid film are silane concentration and silane ratio (APTES:GPTMS).

The contact angle results showed that the best condition for silane hybrid film on galvanneated surface was obtained with the sample S21 ($109,7^\circ$), for 2:1 silane ratio (APTES:GPTMS), 2% silane concentration and 150 min the hydrolysis time, although this variable (V3) is not significant. The most intense and negative effect was obtained for the variable silane concentration (2%, level -1) followed by a less intense positive effect of the silane ratio APTES:GPTMS (2:1, level +1), being both coherent with the highest value for the response variable and the model obtained. All 27 samples treated with the silane hybrid film showed a mean contact angle value higher than SBlank, untreated, of which 8 results (S21, S02, S01, S03, S24, S05, S10 and

S11) with contact angles greater than 90° with hydrophobic characteristics were obtained at lowest concentrations of silane (2%). The most hydrophilic samples tend to the higher concentrations of silane (6%). No significant tendency is observed for the hydrolysis time.

The electrochemical results corroborate wettability results indicating that the silane hybrid film (APTES:GPTMS) improve the galvannealed corrosion resistance.

The SEM images and EDS results indicate that the galvannealed microstructure can contribute with the non-homogeneous film formation due to the surface porosity originating from intermetallic phases and the presence of cracks.

5. ACKNOWLEDGEMENTS

Authors would like acknowledge to FAPESB (Nº BOL0364/2015) for financial support, LAMMA (Environment and Materials Laboratory) of State University of Santa Cruz (Ba, BR) for support, LEC (Corrosion and Electrochemistry Laboratory) of Polytechnic School of the University of São Paulo (SP, BR) for provided wettability tests and CME (Electronic Microscopy Center) of State University of Santa Cruz (BA, BR) for SEM images.

6. BIBLIOGRAPHY

- [1] HEON-YOUNG, H, SEONG-JUN, P, JUN-YUN, K, *et al.*, “Interpretation of the corrosion process of a galvannealed coating layer on dual-phase steel”, *Corrosion Science*, v.53, n.7, pp. 2430-2436, July 2011.
- [2] COOK, D. C., GRANT, R. G. “Iron-zinc phase identification in commercial galvannealed steel coatings”, *Galvatech*, pp. 929-932, Bologna, May 1996.
- [3] ALMEIDA E, MORCILLO M. “Lap-joint corrosion of automotive coated materials in chloride media. Part 3 - Eletrogalvanized steel/galvannealed interface”, *Surface and Coatings Technology*, v.124, n. 1, pp. 44-52, Feb 2000.
- [4] FRANCISCO J S, CAPELOSSI V R, AOKI I V. “Evaluation of a sulfursilane anticorrosive pretreatment on galvannealed steel compared to phosphate under a waterborne epoxy coating”, *Electrochimica Acta*. v.124, n.1, pp. 128-136, April 2014.
- [5] GARZA, L. G., VAN TYNE, C. J. “Friction and formability of “galvannealed” interstitial free sheet steel”, *Journal of Materials Processing Technology*, v.287-188, n.12, pp. 164-168, pp. Jun 2007.
- [6] CHAKRABORTY, A, RAY, R K. “Influence of microstructure and texture on the formability character of industrially produced galvannealed coatings on three interstitial free steels”, *Surface & Coatings Technology*, v.203, n.13, pp. 1756-1764, March 2004.
- [7] QUEIROZ, F. M., COSTA, I. “Electrochemical, chemical and morphological characterization of galvannealed steel coating”, *Surface & Coatings Technology*, v.201, n.16, pp. 7024-7035, May 2007.
- [8] FERNANDES, B. S., SOUZA, K. G. S., AOKI, I. V., *et al.*, “Evaluation of the influence of experimental parameters in the formation of a vinyltrimethoxysilane film on 1010 carbon steel through electrochemical impedance spectroscopy and contact angle techniques”, *Electrochimica Acta*, v.124, n.1, pp. 137-142, April 2014.
- [9] PLUEDDEMANN, E. P. *Silane Coupling Agents*, 2nd ed., Plenum Press, New York, 1991.
- [10] PALANIVEL, V. M. *Modified silane thin films as an alternative to chromates for corrosion protection of AA2024-T3 alloy*, Master Engineering: Materials Science, University of Cincinnati, Suratkal, Índia, 2003.
- [11] KUNST, S. R., BELTRAMI, L. V. R., CARDOSO, H. R. P., *et al.*, “Effect of curing temperature and architectural (monolayer and bilayer) of hybrid films modified with polyethylene glycol for the corrosion protection on tinplate”, *Materials Research*, v. 14, n.4, pp. 1071-1081, July 2014.
- [12] ZOMORODIAN, A., BRUSCIOTTI, F., FERNANDES, A., *et al.*, “Anti-corrosion performance of a new silane coating for corrosion protection of AZ31 magnesium alloy in Hank's solution”, *Surface & Coatings Technology*, v.206, n.21, pp. 4368-4375, June 2012.
- [13] SUBRAMANIAN, V., VAN OOIJ, W. J. “Silane based metal pretreatments as alternatives to chromating”, *Surface Engineering*, v.15, n.2, pp. 168-172, July 2013.
- [14] SERÉ, P. R., DEYÁ, C., ELSNER, C. I., *et al.*, “Corrosion of painted galvanneal steel”, *Procedia Materials Science*, v.8, pp. 1-10, 2015.

- [15] BEXELL, U. *Surface characterisation using ToF-SIMS. AES and XPS of silanes films and organic coatings deposited on metal substrates*. Acta Universitatis Upsaliensis, Comprehensive Summaries of Uppsala Dissertations from the Faculty of Science and Technology, Uppsala, Sweden, 2003.
- [16] CHILD, T. F., VAN OOIJ, W. J. “Application of silane technology to prevent corrosion of metals and improve paint adhesion”, *Transaction of the Institute of Metal Finishing*, v.77, n.2, pp. 64-70, Mat 2017.
- [17] ZHU, D. “Corrosion protection of metals by silane surface treatments”, Thesis of PhD, Department of Materials Science and Engineering of the College of Engineering, University of Cincinnati, United States of America, 2005.
- [18] KUNST, S. R., BELTRAMI, L. V. R., CARDOSO, H. R. P., *et al.*, “Characterization of siloxane-poly(methyl methacrylate) hybrid films obtained on a tinplate substrate modified by the addition of organic and inorganic acids”, *Materials Research*, v.18, n.1, pp. 151-163, Feb.2015.
- [19] CAPELOSSI, V. R., AOKI, I. V. “Influence of sonication on anticorrosion properties of a sulfursilane film doped with Ce (IV) on galvanized steel”, *Progress in Organic Coatings*, v.76, n.5, pp. 791-801, March 2013.
- [20] VAN OOIJ, W. J., ZHU, D., STACY, M., *et al.*, “Corrosion protection properties of organofunctional silanes – An Overview”, *Tsinghua science & technology*, v.10, n.6, pp. 639-664, Dec. 2005.
- [21] MONTEMOR, M. F., FERREIRA, M. G. S. “Analytical characterization of silane films modified with cerium activated nanoparticles and its relation with the corrosion protection of galvanised steel substrates”, *Progress in Organic Coatings*, v.63, n.3, pp. 330-337, Oct. 2008.
- [22] AGUDELO, N. A., PÉREZ, L. D. “Synthesis and characterization of Polydimethylsiloxane end-Modified Polystyrene from Poly(Styrene – co –Vinyltriethoxysilane) copolymers”, *Materials Research*, v.19, n.2, pp. 459-465, Feb. 2016.
- [23] XIANGXUAN, Z., GUOHUA, X., YUAN, G., *et al.*, “Surface Wettability of (3-Aminopropyl) triethoxysilane Self-Assembled Monolayers”, *Journal of Physical Chemistry B*, v.115, n.3, pp.450–454, Jan. 2008.
- [24] SUNKARA V., PARK D.K., HWANG H., *et al.*, “Simple room temperature bonding of thermoplastics and poly(dimethylsiloxane)”, *Lab on a Chip*, v.11, n.5, pp. 962-965, Mar. 2011.
- [25] DUȚU, C. A., VLAD, A., RECKINGER, N., *et al.*, “Tuning the surface conditioning of trapezoidally shaped silicon nanowires by (3-aminopropyl)triethoxysilane”, *Applied Physics Letters*, v.104, n.2, pp. 1-4, Jan. 2014.
- [26] SEMAL, S., BLAKE, T. D., GESKIN, V., *et al.*, “Influence of Surface Roughness on Wetting Dynamics”, *Langmuir*, v.15, n.25, pp. 8765–8770, Oct. 1999.
- [27] FLINK, S., VAN VEGGEL, F. C. J. M., REINHOUDT, D. N. J. “Functionalization of self-assembled monolayers on glass and oxidized silicon wafers by surface reactions”, *Journal of Physical Organic Chemistry*, v.7, n.14, pp. 407-415, Jun. 2001.
- [28] CHOI, S.-H., NEWBY, B.-M. Z. “Suppress polystyrene thin film dewetting by modifying substrate surface with aminopropyltriethoxysilane”, *Surface Science*, v.600, n.6, pp. 1391–1404, Set. 2006.
- [29] WEI, M., BOWMAN, R. S., WILSON, J. L., *et al.*, “Wetting Properties and Stability of Silane-Treated Glass Exposed to Water, Air, and Oil”, *Journal of Colloid and Interface Science*, v.157, n.1, pp. 154–159, Apr. 1993.
- [30] KWOK, D. Y., NEUMANN, A. W. “Contact angle measurement and contact angle interpretation”, *Advances in Colloid and Interface Science*, v.81, n.3, pp.167–249, Set. 1999.
- [31] MA, P.-C., KIM, J. K., TANG, B. Z. “Effects of silane functionalization on the properties of carbon nanotube/epoxy nanocomposites”, *Composites Science and Technology*, v.67, n.14, pp.2965-2972, Nov. 2007.
- [32] WU, S.-Y., YUEN, S.-M., MA, M. C.-C., *et al.*, “Preparation, morphology, and properties of silane-modified MWCNT/epoxy composites”, *Journal of Applied Polymer Science*, v.115, n.6, pp. 3481–3488, Nov. 2009.
- [33] CHEN, H., JACOBS, O., WU, W., *et al.*, “Effect of dispersion method on tribological properties of carbon nanotube reinforced epoxy resin composites”, *Polymer Testing*, v.26, n.3, pp. 351-360, May 2007.
- [34] ZHU, D., VAN OOIJ, W. J. “Corrosion protection of metals by water-based silane mixture of bis-[trimethoxysilylpropyl] amine and vinyltriacetoxysilane”, *Progress in Organic Coatings*, v.49, n.1, pp. 42-53, Jan. 2004.

- [35] FEDEL, M., DRUART, M.-E., OLIVIER, M., *et al.*, “Compatibility between cataphoretic electrocoating and silane surface layer for the corrosion protection of galvanized steel”, *Progress in Organic Coating*, v.69, n.2, pp.118–125, Oct. 2010.
- [36] KERGOAT, L., PIRO, B., SIMON, D. T., *et al.*, “Detection of Glutamate and Acetylcholine with Organic Electrochemical Transistors Based on Conducting Polymer/Platinum Nanoparticle Composites” *Advanced Materials*, v.26, n.32, Jun. 2014.
- [37] HA°KANSSON, A., HAN, S., WANG, S., *et al.*, Effect of (3-Glycidyoxypropyl)Trimethoxysilane (GOPS) on the Electrical Properties of PEDOT:PSS Films”, *Journal of Polymer Science, Part B*, v.55, n.10, pp. 814-820, Mar. 2017.
- [38] DALMORO, V., SANTOS, J.H.Z., ALEMÁN, C., *et al.*, “An assessment of the corrosion protection of AA2024-T3 treated with vinyltrimethoxysilane/(3-glycidyoxypropyl)trimethoxysilane”, *Corrosion Science*, v.92, n.1, pp.200–208, Mar. 2015.
- [39] HOEPFNER, J. C., PEZZIN, S. H. “Functionalization of carbon nanotubes with (3-glycidyoxypropyl)-trimethoxysilane: Effect of wrapping on epoxy matrix nanocomposites”, *Journal of Applied Polymer Science*, v.133, n.47, pp. 44245-44255, Dec. 2016.
- [40] ZAND, R. Z., VERBEKEN, K., FLEXER, V., *et al.*, “Effects of ceria nanoparticle concentrations on the morphology and corrosion resistance of cerium-silane hybrid coatings on electro galvanized steel substrates”, *Materials Chemistry and Physics*, v.145, n.3, pp.450-460, Jun. 2014.
- [41] PANTOJA, M., ABENOJAR, J., MARTÍNEZ, M. A., *et al.*, “Silane pretreatment of electrogalvanized steels: Effect on adhesive properties”, *International Journal of Adhesion & Adhesives*, v.65, n.1, pp. 54–62, Mar. 2016.
- [42] BANDYOPADHYAY, N., JHA, G. K., SINGH, A. K., *et al.*, “Corrosion behaviour of “galvannealed” steel sheet”, *Surface and Coatings Technology*, v.200, n.14-15, pp.4312-4319, Apr. 2006.
- [43] KUNST, S. R., LUDWIN, G. A., CARDOSO, H. R. P., *et al.*, “Hybrid Films with (Trimethoxysilylpropyl) Methacrylate (TMSM), Poly (Methyl methacrylate) PMMA and Tetraethoxysilane (TEOS) Applied on Tinplate”, *Materials Research*, v.17, n.1, pp. 75-81, May 2014.
- [44] FERNANDES, B. S., SOUZA, K. G. S., AOKI, I.V., *et al.*, “Analysis of the formation of a vinyltrimethoxysilane film on 1010 carbon steel using electrochemical techniques”, *Anti-Corrosion Methods and Materials*, v.60, n.5, pp.251-258, Sep. 2013.
- [45] JEYAPRABHA, C, SATHYANARAYANAN, S, VENKATACHARI, G., “Corrosion inhibition of pure iron in 0.5 M H₂SO₄ solutions by ethanalamines”, *Applied Surface Science*, v.246, n.1-3, pp. 108-116, Jun. 2005.
- [46] SIKARWAR, R. S., VELMURUGAN, R., MADHU, V. “Experimental and analytical study of high velocity impact on Kevlar/Epoxy composite plates”, *Central European Journal of Engineering*, v.2, n.4, pp. 638–649, Sep. 2012.
- [47] BOX, G. E. P., HUNTER, W. G., HUNTER, J. S., *Statistics for experimenters – an introduction to design, data analysis and model building*. New York, John Wiley & Sons. 2nd, 1978.
- [48] POROCH-SERITAN, M., CRETESCU, I., COJOCARU, C., *et al.*, “Experimental design for modelling and multi-response optimization of Fe–Ni electroplating process”, *Chemical Engineering Research and Design*, v.96, n.1, pp. 138-149, Feb. 2015.
- [49] MONTGOMERY, D. C., PECK, E. A., VINING, G. G., *Introduction to linear regression analysis*, 5th ed, Wiley-Interscience, 2012.
- [50] TRABELSI, W., DHOUBI, L., TRIKI, E., *et al.*, “An electrochemical and analytical assessment on the early corrosion behaviour of galvanized steel pretreated with aminosilanes”, *Surface & Coatings Technology*, v.192, n.1, pp. 284-290, Mar. 2005.

ORCID

Kleber Gustavo da Silva Souza	https://orcid.org/0000-0001-6070-995X
Fernando Cotting	https://orcid.org/0000-0001-5980-0078
Idalina Vieira Aoki	https://orcid.org/0000-0002-8203-2625
Franco Dani Rico Amado	https://orcid.org/0000-0001-7555-1876
Vera Rosa Capelossi	https://orcid.org/0000-0002-0212-8388